Supplementary Table 1. Clinical characteristics of animals included in the study.

	IA Saline (Ctrl n=16)	**IA LPS 16h (n=13)**	**IA LPS+rIL-1ra 16h (n=6)**	**IA LPS 48h (n=8)**
Maternal age, year ± SD	10 ± 2.1	7 ± 1.8	8.5 ± 2.6	9.9 ± 2.6
Maternal weight (Kg)	8.9 ± 1.5	8.3 ± 1.7	10.3 ± 1.2	9.2 ± 0.8
Median GA at delivery, days [range]	131 [128-136]	132 [128-137]	132 [128-138]	132 [126-137]
Mean birth weight, gram ± SD	332.3 ± 27.2	323.6 ± 36.9	353.9 ± 32.1	319.3 ± 46.5
Fetal gender number (F/M)	8/8	9/4	3/3	1/7

Supplementary Table 2. Clinical characteristics of pregnant women who delivered preterm newborns.

	Preterm chorio negative (n=16)	Preterm chorio positive (n=14)	P value
Maternal age, year ± SD	28.3 ± 2.67	29 ± 7.07	0.8
Median GA at delivery, weeks [range]	32.3 [26.6-35.4]	31.4 [29.1-34]	0.9
Causes of preterm birth			
• **PTL or preterm-PROM**	8/16	12/14	0.06
• **Pre-eclampsia**	3/16	2/14	1.0
• **Other indications**	**5/16**	**0/14**	**0.04**
Antenatal steroid use	11/16	12/14	0.4
Antenatal antibiotics use	**4/16**	**10/14**	**0.03**
Cesarean delivery	10/16	6/14	0.5
The presence of labor	8/16	12/14	0.06
Spontaneous labor	5/8	9/12	0.6
Neonatal male gender	7/16	8/14	0.7
Mean birth weight, gram ± SD	1690 ± 617	1880 ± 375	0.2
White Caucasian race	7/16	9/14	0.3
African-American race	9/16	5/14	0.3

PTL=preterm labor; PIH=pregnancy induced hypertension; HTN=hypertension

P<0.05 between comparators by Fisher's exact test

Supplementary Table 3. List of monoclonal Antibodies used to phenotype chorio-decidua cells by flow cytometry.

mAb	Sample	Manufacturer	Clone	Conjugation
CD45	Rhesus	BDBioscience	D058-1283	PE-CF594
CD45	Human	BDBioscience	HI30	PE-CF594
HLA-DR	Rhesus/Human	Biolegend	L243	Brilliant Violet 570/APC-Cy7
CD3	Rhesus	BDBioscience	SP34-2	APC-Cy7
CD3	Human	BDBioscience	UCHT1	V500
CD14	Rhesus	Thermofisher	TUK4	Pacific Blue
CD14	Human	Biolegend	M5E2	Alexa Fluor 488
CD56	Rhesus/Human	BDBioscience	NCAM16.2	PE-Cy7
CD88	Rhesus	AbD Serotec	P12/1	Alexa Fluor 647
CD66b	Human	BDBioscience	GF105	Alexa Fluor 647
CD19	Rhesus/Human	Biolegend	HIB19	FITC
CD20	Rhesus/Human	Biolegend	2H7	FITC
CD16	Rhesus	BDBioscience	3G8	Alexa Fluor 700
CD63	Rhesus/Human	Biolegend	H5C6	Pacific Blue
CD8α	Rhesus	eBioscience	RPA-T8	eFluor 605
FOXP3	Rhesus	eBioscience	PCH101	eFluor 450
TNFα	Rhesus/Human	BDBioscience	Mab11	Alexa Fluor 700
Live/Dead	Rhesus/Human	Thermofisher		Aqua
Annexin V	Rhesus/Human	BDBioscience		FITC
7aad	Rhesus/Human	BDBioscience		7aad

Supplementary Table 4. List of Rhesus and Human Taqman probes (ThermoFisher Scientific).

IL1B	Rh02621711_m1
IL6	Rh02789322_m1
IL8	Rh02789781_m1
MCP1/CCL2	Rh02621753_m1
TNFA	Rh02789783_m1
IL10	Rh00961619_m1
IFNG	Rh02621721_m1
IDO1	Rh02841203_m1
CXCL10	Rh02788357_m1
CSF3	Rh02825033_m1
S100A8	Rh02913929_m1
CSF3R	Rh01114426_m1
BCL2A1	AIAAZ7T
MCL1	Rh02879361_m1
IDO1	Hs00984148_m1
IL6	Hs00985639_m1
TNFA	Hs99999043_m1
CXCL10	Hs00171042_m1
BCLXL	Hs00236329_m1
MCL1	Hs01050896_m1
BAD	Hs00188930_m1
BAX	Hs00180269_m1
BCL2	Hs00608023_m1
BCL2A1	Hs03405590_m1

Supplementary Figure 1.

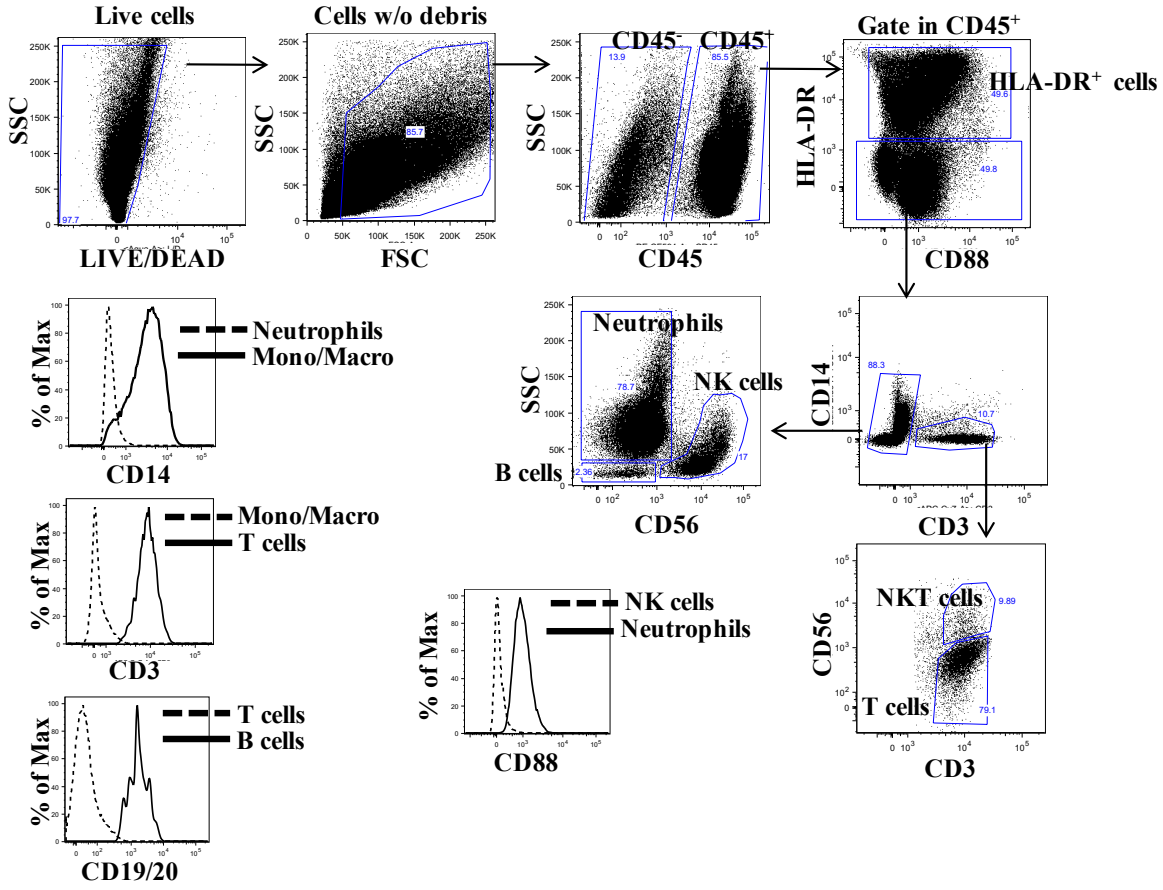

Supplementary Figure 1. Representative gating strategy (n=13) used to characterize the different leukocyte subpopulations in Rhesus chorio-decidua as well as to separate neutrophils and CD45$^-$ cells by FACS sorter. Live cells were first identified by the absence of LIVE/DEAD stain and forward-/side-scatter expression, excluding cell debris. Leukocytes were gated as CD45$^+$ cells. Inside the CD45$^+$ cells, the leukocyte subpopulations were gated as monocytes/macrophages (CD3$^-$ CD14^{high}CD88$^+$HLA-DR$^+$); neutrophils (CD3$^-$CD14^{low}HLADR$^-$CD88$^+$CD56$^-$); NK cells (CD3$^-$CD14$^-$HLA-DR$^-$CD88$^-$CD56$^+$); B cells (CD3$^-$CD14$^-$CD56$^-$CD19/CD20$^+$); T cells (CD14$^-$CD56$^-$CD3$^+$); and NKT cells (CD14$^-$CD3$^+$CD56$^+$). HLA-DR$^+$ cells are mostly CD14$^+$ monocytes/macrophages, but they also contain some CD19/CD20$^+$ B cells. A similar gating strategy was used to characterize human cells, with the only difference that CD66b was used instead of CD88 for neutrophils (not shown).

Supplementary Figure 2.

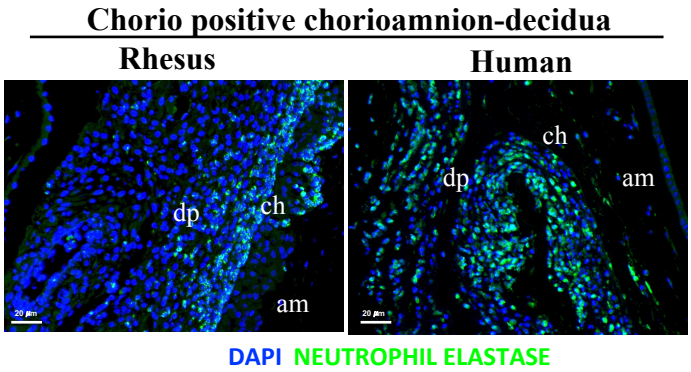

Supplementary Figure 2. Neutrophil recruitment at the maternal-fetal interface is similar both in Rhesus and human in the setting of chorioamnionitis (chorio). Representative immunostaining of Neutrophil Elastase (n=5) in fetal membranes of chorio^{+} samples (am=amnion; ch=chorion; dp=decidua parietalis).

Supplementary Figure 3.

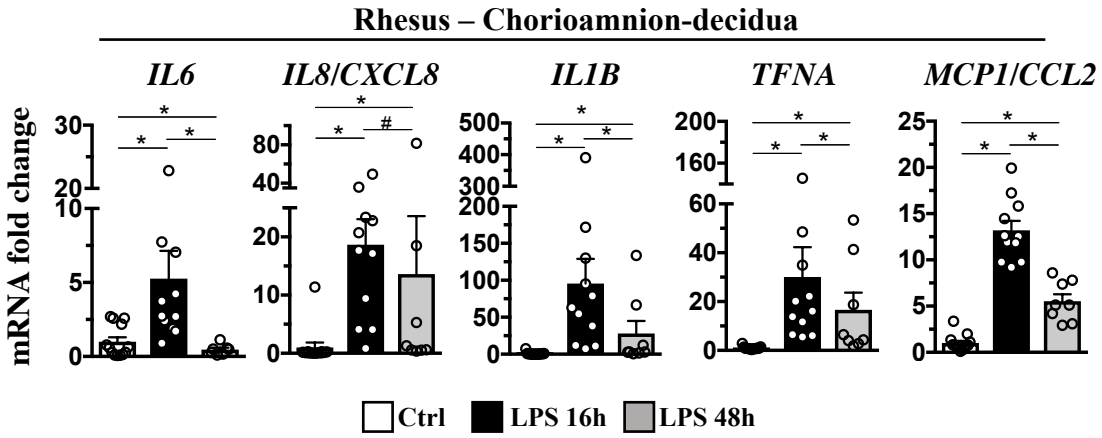

Supplementary Figure 3. Time-course of inflammation induced by IA-LPS injection in chorioamnion-decidua. Intra-amniotic injection of LPS induced a robust inflammation at 16 hours with a subsequent decrease at 48 hours. Histograms represent cytokine mRNAs in the chorioamnion-decidua (CAD) expressed as fold increases over the average value for controls after internally normalizing to the housekeeping 18S RNA. (Ctrl n=13; LPS16h n=11; LPS48h n=8). (Data are mean, SEM. *p<0.05 between comparators; #0.1<p>0.05 between comparators by Mann-Whitney test).

Supplementary Figure 4.

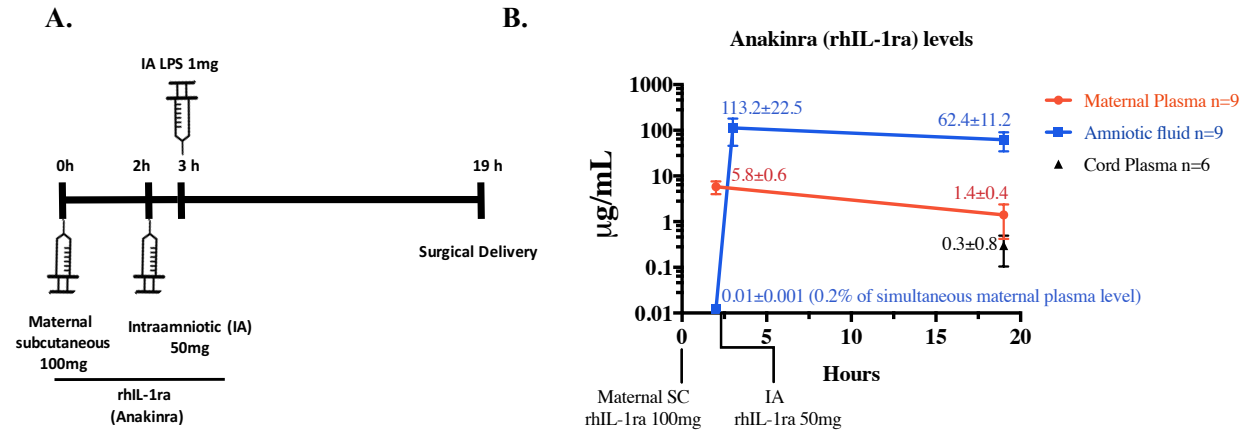

Supplementary Figure 4. **Experimental Schema and Anakinra Pharmacokinetics** (A) Schematic of dosing regimen in ~130d Rhesus macaques (80% gestation). (B) Pharmacokinetics of Anakinra measured by human IL-1ra specific bead-based ELISA. Note the low (0.2%) diffusion of Anakinra from maternal blood to Amniotic fluid (AF) 2h after maternal Subcutaneous (SC) before the AF Anakinra dosing. Also note the slower clearance of Anakinra from the AF compared to maternal plasma. There was a substantial transfer of Anakinra (19h level) to fetal plasma reflecting trans-placental transfer.

Supplementary Figure 5.

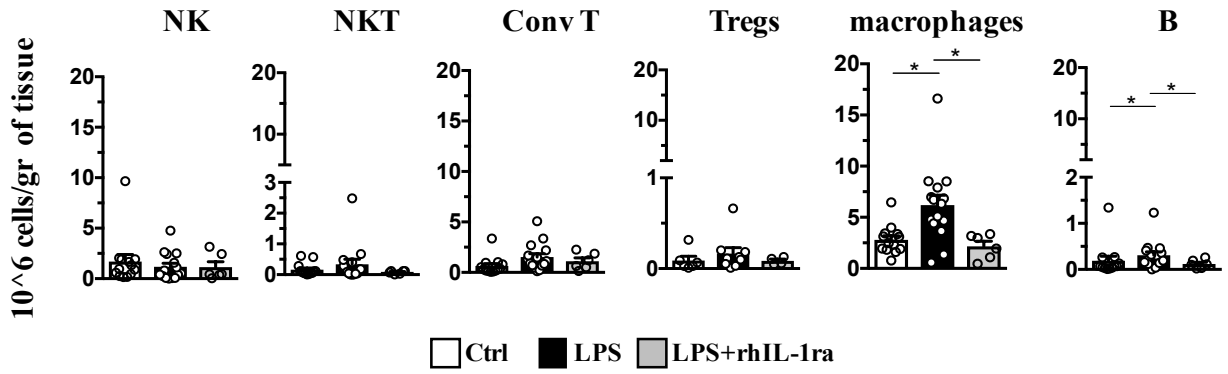

Supplementary Figure 5. IA LPS slightly increased monocyte/macrophage and B-cells in the chorio-decidua in an IL-1 dependent manner. Chorio-decidua cell suspensions were analyzed by multiparameter flow cytometry. IA LPS exposure increased only the number of chorio-decidua monocytes/macrophages and B cells compared to the control animals and rhIL-1ra reverted monocyte/macrophage and B cell numbers to control levels. LPS had no impact on NK, NKT, conventional T-cell or Treg (defined as $CD3^{+}CD8^{-}FOXP3^{+}$ cells) numbers (Ctrl n=11; LPS n=12; LPS+rhIL-1ra n=6) (Data are mean, SEM, *p<0.05 between comparators by Mann-Whitney test).

Supplementary Figure 6.

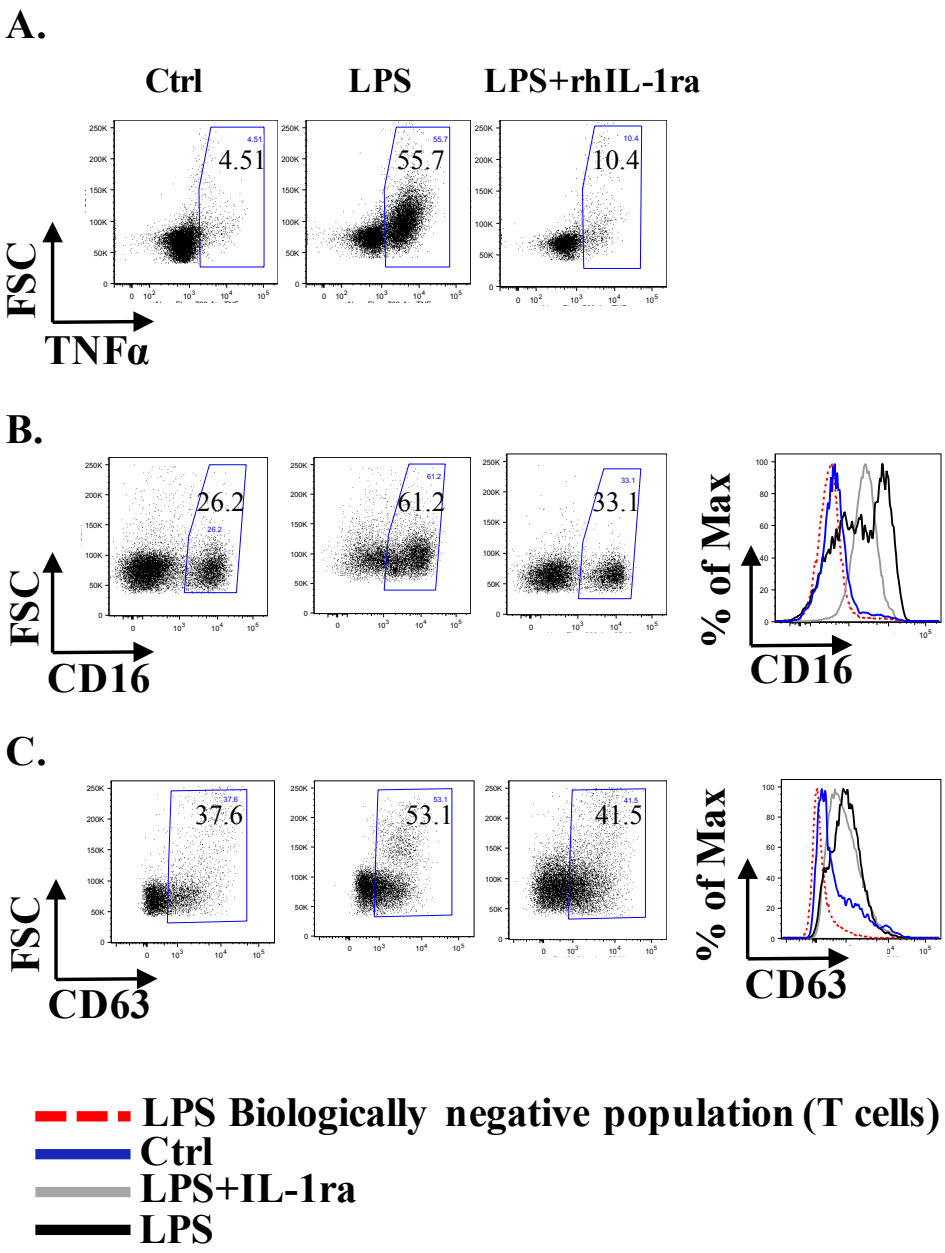

Supplementary Figure 6. Representative dot plots (n=5) showing activation of chorio-decidua neutrophils. Chorio-decidua cell suspension were analyzed by flow cytometry. Frequency of (A) TNFα^{+}, (B) CD16^{+}, and (C) CD63^{+} neutrophils decreased upon rhIL-1ra treatment.

Supplementary Figure 7.

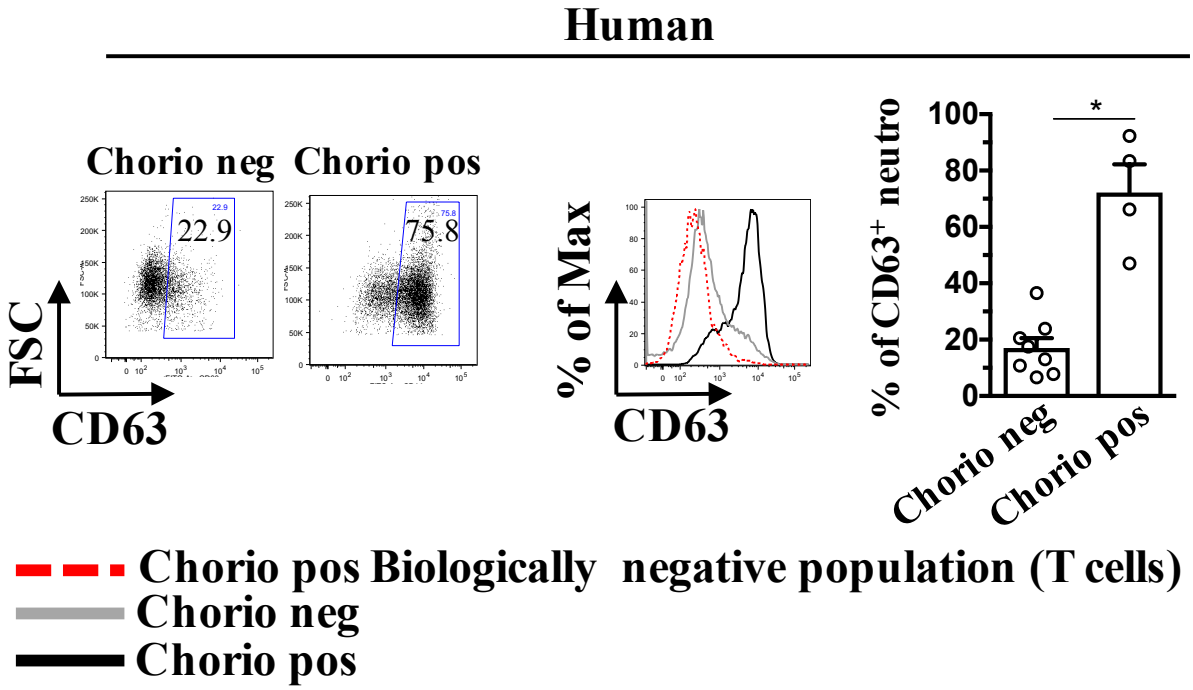

Supplementary Figure 7. Increased CD63 expression in chorio-decidua neutrophils during human chorioamnionitis. Similarly to Rhesus, human chorio-decidua neutrophils from pre-term chorioamnionitis positive samples (n=4) express higher CD63 compared to neutrophils from pre-term chorio negative samples (n=9). (Data are mean, SEM, *p<0.05 between comparators by Mann-Whitney Test).

Supplementary Figure 8.

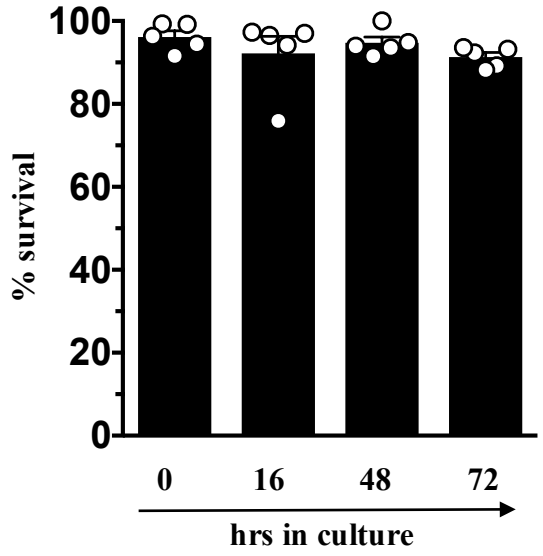

Supplementary Figure 8. Chorio-decidua neutrophil survival over 3 days. Chorio-decidua cells isolated from IA LPS-exposed animals (n=5) were cultured without any stimulation for the time indicated. Chorio-decidua neutrophil survival (Annexin V^-/$7aad^-$) was assessed by flow cytometry. There was minimal loss of survival over 72h of culture (Data are mean, SEM).

Supplementary Figure 9.

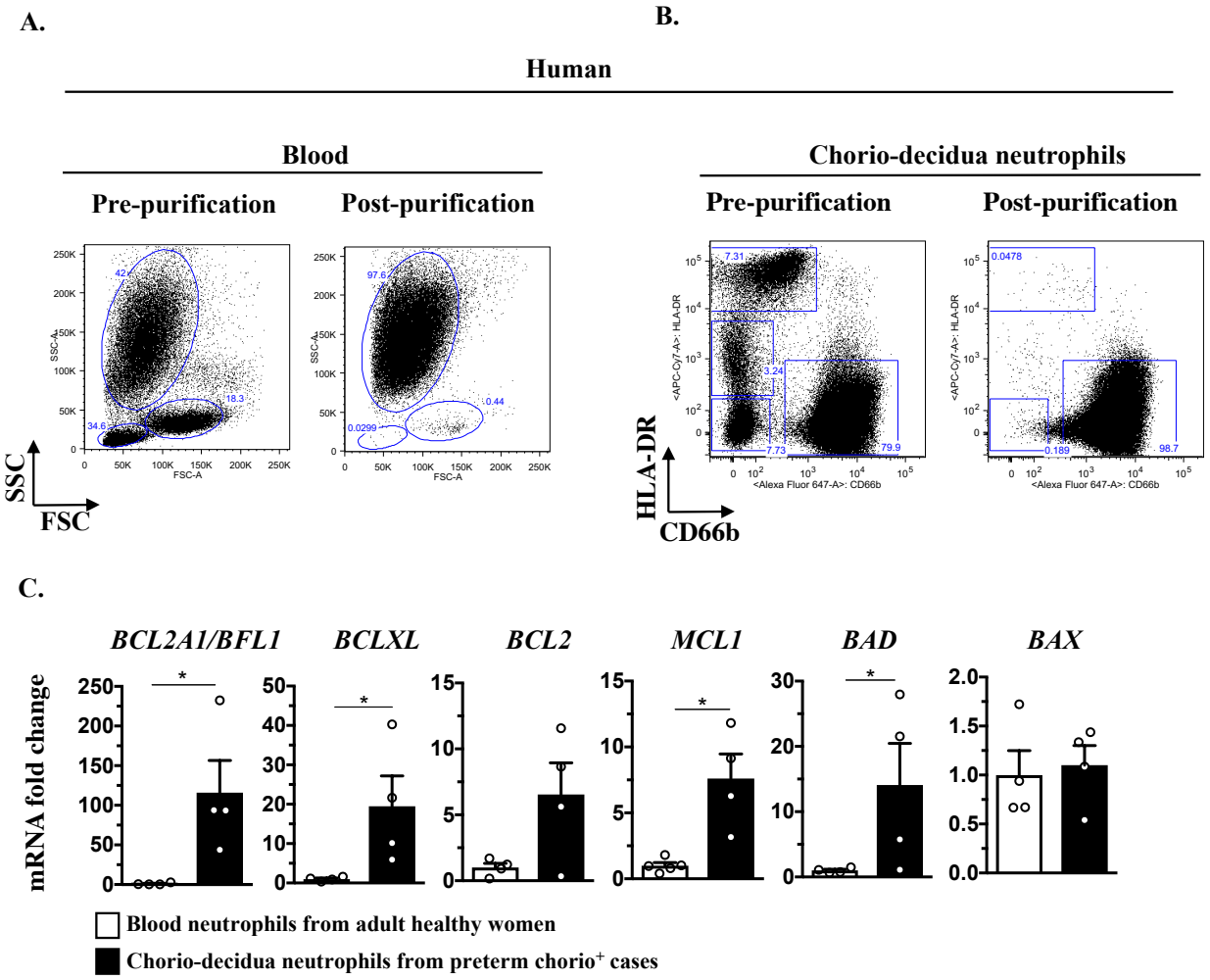

Supplementary Figure 9. Chorioamnionitis induced expression of the pro-survival factor *Bcl2A1/Bfl1* in human chorio-decidua neutrophils (A) Representative dot plots showing pre- and post-purification of human peripheral blood neutrophils. (B) Chorio-decidua neutrophils from human preterm chorioamnionitis positive membranes were isolated by CD66b$^+$ selection. Dot plots represent chorio-decidua cells pre-isolation and post-isolation (similar results were obtained by negative selection, not shown). (C) Human immuno-magnetic bead purified chorio-decidua neutrophils from preterm chorioamnionitis positive cases showed a significant increase of anti-apoptotic *Bcl2A1/Bfl1, Bcl-xl*, and *Mcl-1*, and pro-apoptotic *Bad* compared to blood neutrophils from adult healthy women. (Data are mean, SEM, *p<0.05 between comparators by Mann-Whitney test).

Supplementary Figure 10.

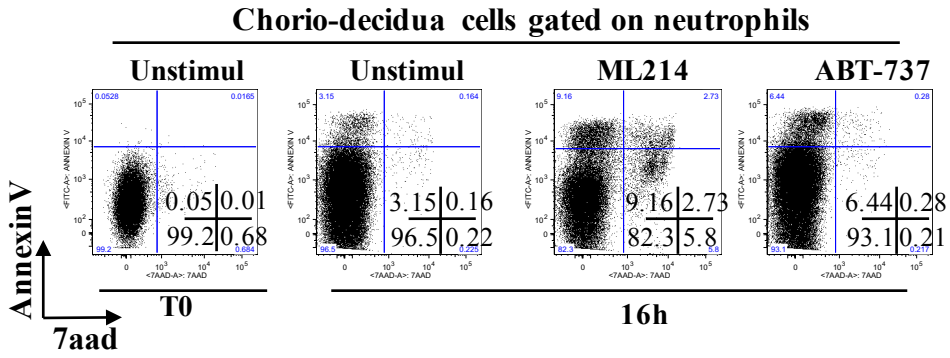

Supplementary Figure 10. Gating strategy for detecting apoptosis in neutrophils. Representative dot plots (n=5-14) showing higher frequency of apoptosis in chorio-decidua cells gated on neutrophils isolated from IA LPS-exposed animals. Neutrophils cultured with ML214 (5μM) had more neutrophils in the upper left + upper right + lower right quadrants while ABT-737 (0.1μM) did not impact chorio-decidua neutrophil apoptosis.